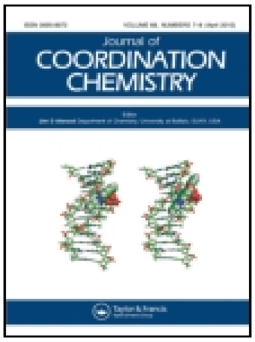

Journal of Coordination Chemistry

ISSN: 0095-8972 (Print) 1029-0389 (Online) Journal homepage: http://www.tandfonline.com/loi/gcoo20

Hydrothermal syntheses, crystal structures, and properties of two new coordination polymers constructed from a flexible pyridinecarboxylate ligand

Guang'en Xing, Yan Zhang, Sufang Zhang & Yanli Dong

To cite this article: Guang'en Xing, Yan Zhang, Sufang Zhang & Yanli Dong (2015) Hydrothermal syntheses, crystal structures, and properties of two new coordination polymers constructed from a flexible pyridinecarboxylate ligand, Journal of Coordination Chemistry, 68:11, 2006-2013, DOI: 10.1080/00958972.2015.1035262

To link to this article: http://dx.doi.org/10.1080/00958972.2015.1035262

Journal of Coordination Chemistry, 2015
Vol. 68, No. 11, 2006–2013, http://dx.doi.org/10.1080/00958972.2015.1035262

Hydrothermal syntheses, crystal structures, and properties of two new coordination polymers constructed from a flexible pyridinecarboxylate ligand

GUANG'EN XING*†, YAN ZHANG†, SUFANG ZHANG† and YANLI DONG‡

†Department of Applied Chemistry, Hengshui University, Hengshui, China
‡College of Sciences, Agricultural University of Hebei, Baoding, China

(*Received 5 November 2014; accepted 11 March 2015*)

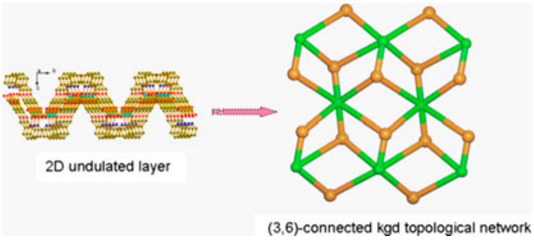

Presented here are two new isomeric coordination polymers, $[Zn(L)]_{2n}\cdot n(H_2O)$ (**1**) and $[Co(L)]_{2n}\cdot n(H_2O)$ (**2**) (H_2L = 5-(pyridin-2-ylmethoxy)-isophthalic acid), which crystallize in orthorhombic, chiral $P2_12_12$ space group and feature 2D undulated layer structure with (3,6)-connected **kgd** topology.

Two new coordination polymers with the same topological structure $[Zn(L)]_{2n}\cdot n(H_2O)$ (**1**) and $[Co(L)]_{2n}\cdot n(H_2O)$ (**2**) (H_2L = 5-(pyridin-2-ylmethoxy)-isophthalic acid) have been hydrothermally synthesized by reactions of metal salts and H_2L. Single-crystal X-ray analyses reveal that **1** and **2** are isostructural and crystallize in orthorhombic chiral $P2_12_12$ space group. These compounds feature 2-D undulated layer structures with (3,6)-connected **kgd** topology, which further extended into a 3-D supramolecular framework via intermolecular hydrogen bonds. In addition, the luminescent properties of **1** and **2** and the magnetic property of **2** were also investigated.

Keywords: Hydrothermal reaction; 5-(Pyridin-2-ylmethoxy)-isophthalic acid; Luminescence; Magnetic

1. Introduction

Design and synthesis of metal–organic frameworks (MOFs) have made achievements owing to their intriguing structural topologies and potential applications in luminescence, catalysis, gas storage, and nonlinear optics [1–5]. Generally, the most effective method for construction of MOFs is hydro(solvo)thermal reactions of metal ions and organic ligands. During

---

*Corresponding author. Email: guangen3157@163.com the process of self-assembly, there are many unpredictable factors, such as pH, reaction temperature, the ratio of metal ions and ligand, solvents, and counter ions that can influence the growth and final structure of MOFs [6–9]. The most crucial components for construction of MOFs are the nature of organic ligand with appropriate flexibility and symmetry and metal ions with fixed coordination number and geometry [10]. Therefore, selection of appropriate organic ligand and metal ion is important for controllable synthesis of MOFs.

5-(Pyridin-2-ylmethoxy)-isophthalic acid (H_2L) as a bifunctional organic ligand has a flexible –CH_2–O– spacer between the pyridyl and phenyl rings. This structure may display various coordination modes and adopt suitable configuration according to the requirement of metal ions in the assembly process. Compared with rigid pyridinecarboxylate ligands, the coordination chemistry of such flexible pyridinecarboxylate ligands is less investigated [11, 12]. In this work, we exploit H_2L as ligand to assemble with Zn(II) or Co(II) ions, obtaining two isostructural compounds, $[Zn(L)]_{2n}\cdot n(H_2O)$ (**1**) and $[Co(L)]_{2n}\cdot n(H_2O)$ (**2**) (H_2L = 5-(pyridin-2-ylmethoxy)-isophthalic acid). Single-crystal X-ray diffraction analyses reveal that these two compounds feature 2-D undulated layered structures with (3,6)-connected **kgd** topology. The luminescence of **1** and magnetism of **2** in the solid state were also investigated.

2. Experimental

2.1. *Materials and instrumentation*

All reagents and solvents employed in this work were commercially available and used without purification. Elemental analyses (C, H, and N) were determined with an elemental Vario EL III analyzer. Powder X-ray diffraction (PXRD) analyses were recorded on a PANalytical X'Pert Pro powder diffractometer with Cu/Kα radiation (λ = 1.54056 Å) with a step size of 0.05°. Circular dichroism (CD) measurements were performed on a MOS-450 spectropolarimeter. Fluorescence spectra of the solid samples were performed on an Edinburgh Analytical instrument FLS920. Magnetic data were obtained with a Quantum Design MPMS XLSQUID magnetometer.

2.2. *Synthesis of $[Zn(L)]_{2n}\cdot n(H_2O)$ (1)*

A mixture of $Zn(NO_3)_2\cdot 6H_2O$ (0.030 g, 0.1 mmol), H_2L (0.025 g, 0.1 mmol), $NaHCO_3$ (0.016 g, 0.2 mmol), and H_2O (10 mL) was placed in a 23 ml Teflon-lined stainless steel reactor under autogenous pressure at 150 °C for 60 h, and then cooled to room temperature slowly. Colorless block crystals (0.0102 g) were obtained in 34% yield based on $Zn(NO_3)_2\cdot 6H_2O$. Anal Calcd for $C_{28}H_{20}N_2O_{11}Zn_2$ (691.24): C, 48.61; H, 2.89; N, 4.05%. Found: C, 48.58; H, 2.92; N, 4.02%.

2.3. *Synthesis of $[Co(L)]_{2n}\cdot n(H_2O)$ (2)*

A mixture of $Co(NO_3)_2\cdot 6H_2O$ (0.030 g, 0.1 mmol), H_2L (0.025 g, 0.1 mmol), $NaHCO_3$ (0.016 g, 0.2 mmol), and H_2O (10 mL) was placed in a 23 ml Teflon-lined stainless steel reactor under autogenous pressure at 150 °C for 60 h, and then cooled to room temperature slowly. Purple block crystals (0.0096 g) were obtained in 32% yield based on

$Co(NO_3)_2 \cdot 6H_2O$. Anal Calcd for $C_{28}H_{20}N_2O_{11}Co_2$ (678.32): C, 49.53; H, 2.95; N, 4.13%. Found: C, 49.51; H, 2.92; N, 4.12%.

2.4. *X-ray crystallography*

Suitable single crystals of 1 and 2 were carefully selected under an optical microscope and glued to thin glass fibers. Structural measurements were performed with a computer-controlled mercury CCD diffractometer with graphite-monochromated Mo–Kα radiation (λ = 0.71073 Å) at T = 293(2) K. Absorption corrections were made using SADABS [13]. The structures were solved by direct methods and refined by full-matrix least-squares on F^2 using SHELXL–97 [14]. All non-hydrogen atoms were refined anisotropically. The hydrogens attached to organic ligands were geometrically placed and refined using a riding model. Crystal data as well as details of data collection and refinements of **1** and **2** are summarized in table 1; selected bond lengths and angles are given in table 2.

3. Results and discussion

3.1. *Description of structure*

Single-crystal X-ray structural analyses reveal that 1 and **2** are isostructural and crystallize in the chiral $P2_12_12$ space group with the flack parameters of 0.0195 and 0.0411, respectively. Only the structure of **1** is selected as representative and described in detail. The asymmetric unit of **1** contains one Zn(II), one L^{2-} and half of a free water molecule. As shown in figure 1, each Zn(II) is coordinated with four carboxylate oxygens (O2, O1a, O4b and O5b) from three different L^{2-} ligands and one nitrogen (N1c) from another L^{2-}, displaying a distorted square pyramidal geometry. The Zn–O distances are 1.987(3)–2.471

Table 1. Crystal data and structure refinements for **1** and **2**.

	1	**2**
Formula	$C_{28}H_{20}N_2O_{11}Zn_2$	$C_{28}H_{20}N_2O_{11}Co_2$
Fw	691.24	678.32
Crystal system	Orthorhombic	Orthorhombic
Space group	$P2_12_12$	$P2_12_12$
a (Å)	10.079(2)	10.052(3)
b (Å)	15.624(3)	15.422(4)
c (Å)	8.8786(18)	9.011(2)
α (°)	90.00	90.00
β (°)	90.00	90.00
γ (°)	90.00	90.00
Volume (Å^3)	1398.2(5)	1397.0(6)
Z	2	2
Density (calculated)	1.642	1.613
Abs. coeff. (mm^{-1})	1.781	1.253
Total reflections	8885	8719
Unique reflections	2432	2417
Goodness of fit on F^2	0.974	1.025
Final R indices [$I > 2\text{sigma}(I^2)$]	$R = 0.0334$, $wR_2 = 0.0832$	$R = 0.0292$, $wR_2 = 0.0818$
R (all data)	$R = 0.0407$, $wR_2 = 0.1105$	$R = 0.0363$, $wR_2 = 0.1059$

Table 2. Selected bond lengths (Å) and angles (°) for **1** and **2**.

Compound **1**			
Zn(1)–O(5)^a	1.987(3)	Zn(1)–O(2)	2.014(3)
Zn(1)–O(1)^b	2.019(3)	Zn(1)–N(1)^c	2.044(3)
Zn(1)–O(4)^a	2.471(3)	O(5)^a–Zn(1)–O(1)^b	104.29(11)
O(2)–Zn(1)–O(1)^b	107.89(11)	O(5)^a–Zn(1)–N(1)^c	135.49(13)
O(2)–Zn(1)–N(1)^c	112.64(13)	O(1)^b–Zn(1)–N(1)^c	98.52(12)
O(5)^a–Zn(1)–O(2)	96.03(13)	O(5)^a–Zn(1)–O(4)^a	57.79(12)
O(2)–Zn(1)–O(4)^a	151.49(11)	O(1)^b–Zn(1)–O(4)^a	90.90(11)
N(1)^c–Zn(1)–O(4)^a	84.50(12)		
Compound **2**			
Co(1)–O(4)^a	2.026(3)	Co(1)–O(3)^b	2.026(2)
Co(1)–O(1)	2.037(3)	Co(1)–N(1)^c	2.054(3)
Co(1)–O(2)	2.312(3)	O(4)^a–Co(1)–O(3)^b	104.75(10)
O(4)^a–Co(1)–O(1)	93.87(11)	O(3)^b–Co(1)–O(1)	103.53(10)
O(4)^a–Co(1)–N(1)^c	113.23(12)	O(3)^b–Co(1)–N(1)^c	96.88(10)
O(1)–Co(1)–N(1)^c	140.53(12)	O(4)^a–Co(1)–O(2)	152.60(10)
O(3)^b–Co(1)–O(2)	89.83(9)	O(1)–Co(1)–O(2)	59.77(10)
N(1)^c–Co(1)–O(2)	87.25(11)		

Note: Symmetry codes for **1** (a) $x - 1, y, z$; (b) $-x + 1, -y + 2, z$; (c) $x - 1/2, -y + 3/2, -z + 1$; for **2** (a) $x + 1, y, z$; (b) $-x + 1, -y - 1, z$; (c) $x + 1/2, -y - 1/2, -z + 3$.

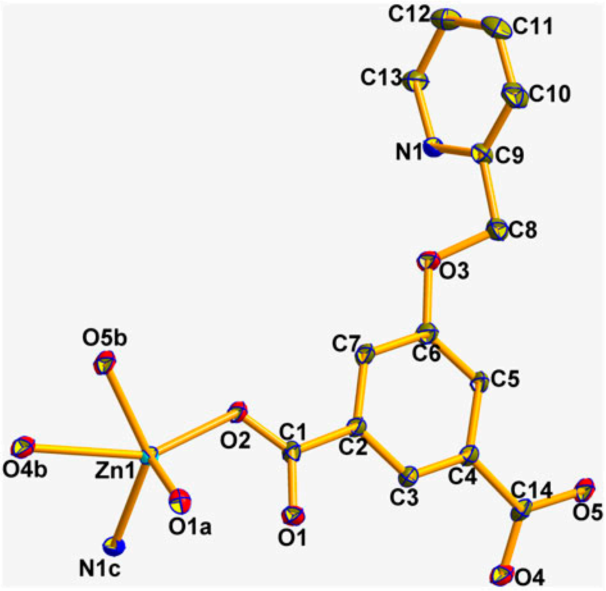

Figure 1. An ORTEP drawing of the asymmetric unit of **1** (30% thermal ellipsoids). Symmetry codes: (a) $x, -y + 1/2, z + 1/2$; (b) $-x + 2, y - 1/2, -z + 3/2$; (c) $-x + 2, y + 1/2, -z + 3/2$; (d) $-x + 3, y + 1/2, -z + 5/2$.

(3) Å and the Zn–N distance is 2.044(3) Å, comparable to those of $[Zn_4(\mu_4\text{-}O)(L)_2(H_2O)_3]_n$ (L^{3-} = biphenyl-3,4,5-tricarboxylate anion) reported by Bu and co-workers [15]. (For **2**, the Co–O distances are 2.026(3)–2.312(3) Å and the Co–N distance is 2.054(3) Å, comparable to that of reported Co(II) compounds [16]). Each L^{2-} links four Zn(II) ions in μ_4-(η^2-O‴, O‴), O, O′, N coordination. Two symmetry-related Zn(II) ions are bridged by two carboxylate groups from two different L^{2-} ligands, generating a dinuclear $[Zn_2(COO)_4]$ building

subunit with Zn···Zn distance of 3.9862(8) Å, which is longer than that of the reported dinuclear [$Zn_2(COO)_4$] cluster [17]. These dinuclear [$Zn_2(COO)_4$] subunits were further connected by carboxylate of L^{2-} into a 1-D 2_1 right-handed helical chain (figure S1, see online supplemental material at http://dx.doi.org/10.1080/00958972.2015.1035262). These 1-D helical chains are further bridged by L^{2-} into a 2-D layer extending along the *ab* plane [figure 2(a)]. The chirality of **1** and **2** originate from the helical chain. Compared with the reported Zn(II) and Co(II) compounds based on isophthalate ligands, we found that the introduction of pyridine into the isophthalate may facilitate the generation of 2-D coordination polymer [18–20]. Viewing along the crystallographic *a* axis, this 2-D layer is undulated [figure 2(b)]. In this 2-D layer, each L^{2-} links three different dinuclear [$Zn_2(COO)_2$] subunits and each dinuclear [$Zn_2(COO)_2$] subunit is surrounded by six different L^{2-} ligands. From topology, the L^{2-} and dinuclear [$Zn_2(COO)_2$] subunit can be reduced into 3-, 6-connected nodes, respectively (figure S2); therefore, the 2-D layer of **1** represents a (3,6)-connected **kgd** topology with the Schläfli symbol of $\{4^3\}_2\{4^6.6^6.8^3\}$ [figure 2(c)]. There are also weak hydrogen bonding interactions between adjacent 2-D sheets. Packing of these 2-D sheets directed by intermolecular hydrogen bonds (C10···O4 = 3.49 Å, ∠C10H10AO4 = 161° and C13···O1 = 3.15 Å, ∠C13H13AO1 = 120°) resulted in a 3-D supramolecular framework [figure 2(d)].

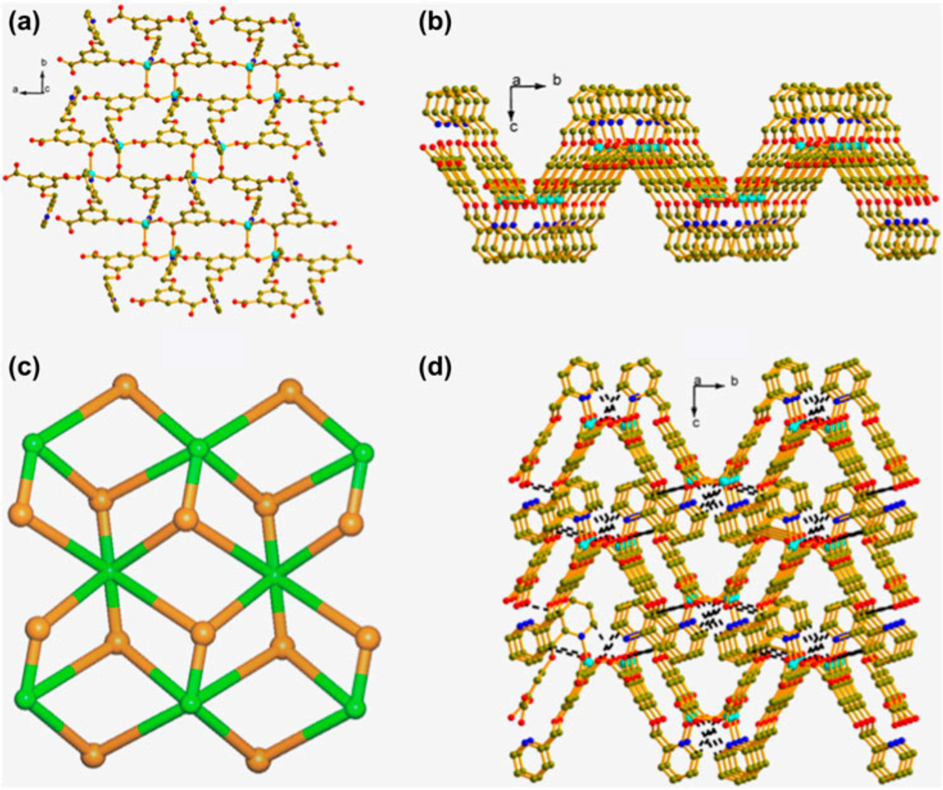

Figure 2. (a) 2-D layer structure of **1** viewed along the *c* axis. (b) 2-D undulated layered structure viewed along the *a* axis. (c) Schematic representation of (3,6)-connected topological network for **1**. (d) 3-D supramolecular framework connected by intermolecular hydrogen bonds (black dotted lines represent hydrogen bonds).

3.2. *PXRD patterns*

PXRD experiments for **1** and **2** were performed to verify whether the bulk samples of **1** and **2** are in pure phase. As shown in figure 3(a) and (b), the experimental patterns match well with the simulated patterns based on the single-crystal diffraction data, confirming that **1** and **2** are pure phases.

3.3. *CD spectra of 1 and 2*

Solid-state CD measurements were done to investigate the chiral nature of 1 and **2**. As shown in figure S3, the positive Cotton effects indicate that the bulk samples of **1** and **2** are homochiral.

3.4. *Photoluminescent properties of 1 and 2*

The solid-state photoluminescent properties of **1** and **2** were investigated at room temperature. As shown in figure 4(a), 1 shows strong luminescent emission at 510 nm (λ_{ex} = 345 nm) and **2** has a luminescent emission band at 554 nm (λ_{ex} = 350 nm) [figure 4(a)]. In order to further ascertain the luminescence origin of **1** and **2**, the luminescence of free H_2L was also studied at the same conditions. Unexpectedly, there is no obvious emission for free H_2L in the visible light range. Therefore, the luminescent emission of **1** and **2** can be tentatively assigned to ligand-to-metal charge transfer [11, 12].

3.5. *Magnetism of 2*

Variable-temperature magnetic susceptibility for **2** was performed on powder samples from 2–300 K under an applied magnetic field of 1000 Oe [figure 4(b)]. The $\chi_M T$ value at 300 K is 2.31 $cm^3 \cdot mol^{-1} \cdot K$, higher than the spin-only value (1.87 $cm^3 \cdot mol^{-1} \cdot K$) for one uncoupled tetrahedral high-spin Co(II) ($S = 3/2$, $g = 2$), which is comparable to the previously reported mononuclear tetrahedral Co(II) compounds [16]. Upon cooling, the $\chi_M T$ value drops very slowly from 2.31 $cm^3 \cdot mol^{-1} \cdot K$ at 300 K to 2.25 $cm^3 \cdot mol^{-1} \cdot K$ at 50 K, and then decreases steeply to 1.47 $cm^3 \cdot mol^{-1} \cdot K$ at 2 K. The magnetic susceptibility of **2**

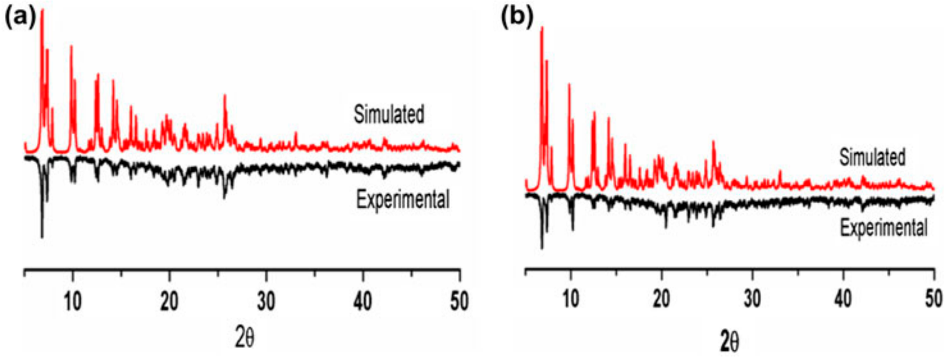

Figure 3. The PXRD patterns (a) for **1** and (b) for **2**.

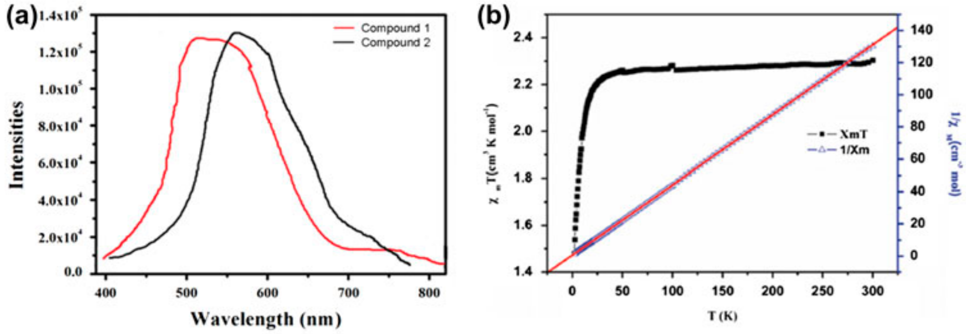

Figure 4. (a) Fluorescent emission spectra of **1** and **2** in the solid state at room temperature. (b) Plots of $\chi_M T$ and $\chi_M{}^{-1}$ *vs.* T for **2**; the solid line represents Curie–Weiss fitting.

above 50 K fits well to the Curie–Weiss law $\chi_M = [C/(T - \theta)]$, giving $C = 2.31\ \mathrm{m}^3\cdot\mathrm{mol}^{-1}\cdot\mathrm{K}$ and $\theta = -1.296$ K. The negative Weiss constant (θ) indicates weak antiferromagnetic exchange between Co(II) ions [21].

4. Conclusion

Two new compounds based on flexible pyridinecarboxylate have been obtained under hydrothermal conditions. These two compounds are isostructural and feature 2-D layered structures with 6-connected **kgd** topology. This work shows that the H_2L (5-(pyridin-2-yl-methoxy)-isophthalic acid) bridge metal ions into 2-D layered structures. Further work about new functional coordination polymers based on H_2L ligand is under way.

Supplementary material

CCDC Nos. 1023888-1023889 contain the supplementary crystallographic data for this paper. These data can be obtained free of charge at www.ccdc.cam.ac.uk/conts/retrieving.html [or from the Cambridge Crystallographic Data Centre, 12 Union Road, Cambridge CB2 1EZ, UK; Fax: (internat.) +44 1223/336 033; E-mail: deposit@ccdc.cam.ac.uk].

Disclosure statement

No potential conflict of interest was reported by the authors.

Funding

This work was supported by the Natural Science Foundation of Hebei Province of China [grant number F2013111006].

References

[1] R.X. Yao, X. Xu, X.M. Zhang. *Chem. Mater.*, **24**, 303 (2012).
[2] S.S. Kaye, A. Dailly, O.M. Yaghi, J.R. Long. *J. Am. Chem. Soc.*, **129**, 14176 (2007).
[3] H.X. Zhang, H.R. Fu, H.Y. Li, J. Zhang, X.H. Bu. *Chem. Eur. J.*, **19**, 11527 (2013).
[4] D. Sun, D.F. Wang, X.G. Han, N. Zhang, R.B. Huang, L.S. Zheng. *Chem. Commun.*, **47**, 746 (2011).
[5] B.L. Chen, L.B. Wang, F. Zapata, G.D. Qian, E.B. Lobkovsky. *J. Am. Chem. Soc.*, **130**, 6718 (2008).
[6] Y.P. He, Y.X. Tan, J. Zhang. *J. Mater. Chem. C*, **2**, 4436 (2014).
[7] X. Zhang, Y.Y. Huang, Y.G. Yao. *J. Mol. Struct.*, **1024**, 146 (2012).
[8] P.X. Yin, J. Zhang, Y.Y. Qin, J.K. Cheng, Z.J. Li, Y.G. Yao. *CrystEngComm*, **13**, 3536 (2011).
[9] J.D. Lin, J.W. Cheng, S.W. Du. *Cryst. Growth Des.*, **8**, 3345 (2008).
[10] X. Zhang, J.X. Yang, J. Zhang, J.K. Cheng, M.L. Sun, Y.G. Yao. *Inorg. Chem. Commun.*, **14**, 986 (2011).
[11] X. Zhang, J.K. Cheng, P.X. Yin, Y.G. Yao. *J. Mol. Struct.*, **990**, 1 (2011).
[12] X. Zhang, J.K. Cheng, F. Chen, M.L. Sun, Y.G. Yao. *Inorg. Chem. Commun.*, **14**, 358 (2011).
[13] G.M. Sheldrick. *SADABS*, University of Göttingen, Göttingen (1996).
[14] G.M. Sheldrick. *SHELXS 97, Program for Solution of Crystal Structures*, University of Göttingen, Göttingen (1997).
[15] X.Z. Bu, Z.W. Wei, C.H. Zhang, S.F. Ren. *Inorg. Chem. Commun.*, **48**, 158 (2014).
[16] X.G. Guo, W.B. Yang, X.Y. Wu, Q.-K. Zhang, L. Lin, R.M. Yu, C.Z. Lu. *CrystEngComm*, **15**, 3654 (2013).
[17] L.Y. Qiao, X. Zhang, J.X. Yang, Z.J. Li, Y.G. Yao. *Chin. Struct. Chem.*, **30**, 1006 (2011).
[18] Y.H. Wen, R.T. Dou, K. Yao, G.F. Xu. *J. Coord. Chem.*, **68**, 38 (2015).
[19] H.Y. Lin, J. Luan, X.L. Wang, G.C. Liu, A.X. Tian, J.W. Zhang. *J. Coord. Chem.*, **68**, 71 (2015).
[20] K.H. Wang, E.J. Gao. *J. Coord. Chem.*, **67**, 563 (2014).
[21] G.P. Yang, B. Liu, L. Hou, P. Liu, B. Liu, Y.Y. Wang, Q.Z. Shi. *Inorg. Chem. Commun.*, **14**, 805 (2011).